

Conference on Assembly Technologies and Systems

## Position Identification in Force-Guided Robotic Peg-in-Hole Assembly Tasks

Ibrahim F. Jasim<sup>a,\*</sup>, Peter W. Plapper<sup>a</sup>, Holger Voos<sup>a</sup><sup>a</sup>*Faculty of Science, Technology, and Communication, University of Luxembourg, L-1359 Luxembourg*\* Corresponding author. Tel.: +352-4666-44-5353; fax: +352-4666-44-5200. E-mail address: [ibrahim.jasim@uni.lu](mailto:ibrahim.jasim@uni.lu)

### Abstract

Position uncertainty is inevitable in many force-guided robotic assembly tasks. Such uncertainty can cause a significant delay, extra energy expenditure, and may even result in detriments to the mated parts or the robot itself. This article suggests a strategy for identifying the accurate hole position in force-guided robotic peg-in-hole assembly tasks through employing only the captured wrench (the Cartesian forces and torques) signals of the manipulated. In the framework of using the Contact-State (CS) modeling for such robotic tasks, the identification of the hole position is realized through detecting the CS that corresponds for the phase of the peg-on-hole, that is the phase in which the peg is located precisely on the hole. Expectation Maximization-based Gaussian Mixtures Model (EM-GMM) CS modeling scheme is employed in detecting the CS corresponding for the peg-on-hole phase. Only the wrench signals are used in modeling and detecting the phases of the assembly process. The considered peg-in-hole assembly process starts from free space and as soon as the peg touches the environment with missing the hole, a spiral search path is followed that would survey the whole environment surface. When the CS of the peg-on-hole is detected, the hole position is identified. Experiments are conducted on a KUKA Lightweight Robot (LWR) doing typical peg-in-hole assembly tasks. Multiple hole positions are considered and excellent performance of the proposed identification strategy is shown.

© 2014 The Authors. Published by Elsevier B.V. This is an open access article under the CC BY-NC-ND license

[\(http://creativecommons.org/licenses/by-nc-nd/3.0/\)](http://creativecommons.org/licenses/by-nc-nd/3.0/).

Selection and peer-review under responsibility of the International Scientific Committee of 5th CATS 2014 in the person of the Conference

Chair Prof. Dr. Matthias Putz [matthias.putz@iwu.fraunhofer.de](mailto:matthias.putz@iwu.fraunhofer.de)**Keywords:** Force-guided robots; peg-in-hole assembly; position uncertainty; robotic assembly;

### 1. Introduction

Force-guided robotic assembly is desired in many situations like occluded parts assembly, unclean industrial environment, variable illumination cases, and other situations that make the vision systems useless. The realization of such robot systems requires adding control and recognition skills that empower the robot in having an abstract knowledge about its environment and handle possible uncertainties efficiently.

One of the crucial elements of realizing force-guided robotic assembly is the accommodation of possible position uncertainty that would add a significant performance limitation if not well addressed. In [1], the authors proposed a search strategy for peg-in-hole assembly tasks that can accommodate the hole position uncertainty by using blind search within a certain circular area of a specific radius. The

notion of six dimensional contact hyper-surface was employed in order to accommodate the position uncertainty in a peg-in-hole assembly process and improved results were obtained [2]. Particle filter was efficiently used in localizing the hole position along with accommodating the high computational cost resulted from large dimensional data [3]. In [4,5], Kim *et.al.* proposed a strategy of finding the shape of the environment using the wrench (the Cartesian forces and torques) signals of the manipulated object and the accommodation of the hole position uncertainty would be feasible.

Despite the promising performance reported in [3,4], the vast computational time and cost of determining the environment may hinder the implementation of such a position search strategy. Inspired from a blindfolded human behavior in finding a hole position, in this article we rely on the notion

of Contact-State (CS) modeling and propose a hole position identification strategy that uses the captured wrench readings of the manipulated object. The Expectation Maximization-based Gaussian Mixtures Model (EM-GMM) CS recognition scheme proposed in [6] and a programmed spiral search path (in case of position uncertainty) are employed in building the proposed hole position identification algorithm.

The rest of the article is organized as follows; in section 2 force-guided robotic peg-in-hole assembly task is described. Section 3 explains the proposed hole position identification algorithm. Experimental validation is detailed in section 4 and the concluding remarks are summarized in section 5.

## 2. Force-Guided Robotic Peg-in-Hole Assembly Tasks

Suppose that we are given the robotic peg-in-hole assembly task shown in Fig. 1. One can see that it is composed of three phases; phase 1 in which the robot is in free space, phase 2 in which the peg is sliding on the surface of the environment and searching for the hole, and phase 3 in which the peg is located straight on the hole (peg-on-hole phase). Phases 1 and 3 always happen when it is required to insert the peg into the hole. However, phase 2 happens when the peg misses the hole. Therefore, for the case of missing the hole, identification of the new hole position is required so that one can avoid the assembly process interruption or possible detriments.

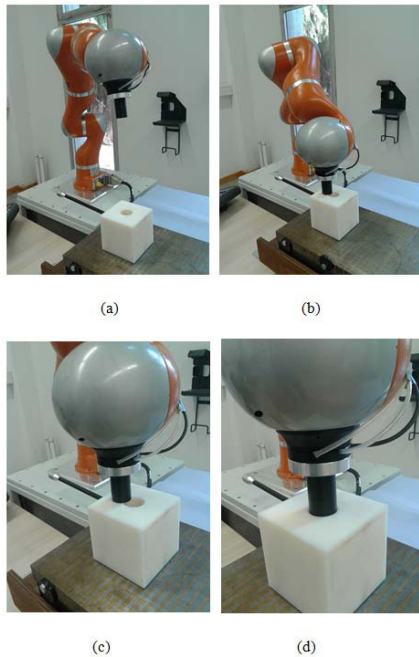


Fig. 1. Force-guided robotic peg-in-hole assembly tasks: (a) Phase 1 (free space); (b) Phase 2; (c) Zoomed image of phase 2; (d) Phase 3.

Consider that the Cartesian force signals of the manipulated object to be:

$$F = [f_x, f_y, f_z] \quad (1)$$

Assume that the corresponding torque signals to be:

$$T = [\tau_x, \tau_y, \tau_z] \quad (2)$$

One can combine (1) and (2) in a vector to obtain the wrench signal of the manipulated object as:

$$w = [f_x, f_y, f_z, \tau_x, \tau_y, \tau_z] \quad (3)$$

The main objective of this article is to use the wrench signals described in (3) for identifying the hole position of Fig. 1 when the peg misses the hole during the insertion process.

## 3. Hole Position Identification Strategy

In order to precisely identify the hole position, we need to add the CS recognition skills and program the robot to move in a certain search path in case the peg misses the hole. Therefore, in the following two subsections both items will be detailed so that the proposed hole identification strategy explained in section 3.3 would be feasible.

### 3.1. Contact-State (CS) Modeling

In the framework of CS modeling, one would aim to use the captured wrench signals (3) in detecting the different phases of the peg-in-hole assembly process. Expectation Maximization-based Gaussian Mixtures Model (EM-GMM) CS modeling scheme is considered one of the most efficient approaches in detecting the different CS phases in force-guided robotic assembly tasks [6]. The superiority of the EM-GMM CS modeling scheme stems from the use of the Gaussian Mixtures Model (GMM) in modeling the likelihood of the captured signals and the employment of the Expectation Maximization (EM) algorithm in finding the optimal parameters that fit the given data to the developed models. Thus, the non-stationary behavior, the signals abnormal distribution, of the captured signals is accommodated that result in an optimal modeling performance.

Consider the wrench signal (3) and suppose that each sample of this vector belongs to one of the phases  $y_k = \{c_1, c_2, \dots, c_C\}$ . One can say that  $w(k)$  belongs to  $c_i$  implies that:

$$p(w(k) | c_i) p(c_i) \geq p(w(k) | c_j) p(c_j) \quad (4)$$

for  $i \neq j$ . The best approximation of the likelihood function  $p(w(k) | c_i)$  results in the best modeling of  $w(k)$  using (4). GMM can be used in building the likelihood  $p(w(k) | c_i)$  that would result in efficient modeling of the captured signals [7]. The GMM likelihood of  $p(w(k) | c_i)$  can be described as:

$$p(w(k) | c_i; \theta) = \sum_{q=1}^M \omega_q N_q(w(k), \mu_q, \Sigma_q) \quad (5)$$

$M$  is the total number of Gaussian mixtures;  $\theta_q = (\omega_q, \mu_q, \Sigma_q)$  is

the GMM parameter vector;  $\omega_q$ ,  $\mu_q$ , and  $\Sigma_q$  are the  $q^{th}$  Gaussian component weight, mean, and covariance respectively.  $N_q(w(k), \mu_q, \Sigma_q)$  is the  $q^{th}$  Gaussian distribution that is characterized by:

$$N_q(w(k), \mu_q, \Sigma_q) = \frac{1}{2\pi^{D/2} |\Sigma_q|^{\frac{1}{2}}} \exp\left(-\frac{1}{2}(w(k) - \mu_q)^T \Sigma_q^{-1} (w(k) - \mu_q)\right) \quad (6)$$

$|\Sigma_q|$  is the determinant of  $\Sigma_q$  and  $D$  is the width of the considered vector, i.e.  $D=6$  for the case of the wrench vector. Suppose that  $\theta = [\theta_1, \theta_2, \dots, \theta_M]^T$ . One can use the EM algorithm in finding the optimal parameters of  $\theta$ . In order to summarize the EM algorithm, consider the log-likelihood to be:

$$L(X | c_i; \theta) = \sum_{n=1}^N \ln(p(x_n | c_i; \theta)) \quad (7)$$

The parameters  $\theta$  that maximizes (7) can be described as:

$$\theta = \arg(\max_{\theta} \{L(X | c_i; \theta)\}) \quad (8)$$

The EM algorithm is employed in solving the optimization problem of (8) and as explained below:

**Step 1:** Initialize the parameter vector  $\theta_q = (\omega_q, \mu_q, \Sigma_q)$ . Initialize the convergence parameters  $\varepsilon$  and  $\delta$ .

**Step 2:** (E-Step) Use the current parameter vector  $\theta_q$  for computing the responsibilities that are:

$$\gamma_n = \frac{\omega_q N_q(x_n, \mu_q, \Sigma_q)}{\sum_{q=1}^M \omega_q N_q(x_n, \mu_q, \Sigma_q)} \quad (9)$$

**Step 3:** (M-Step) Re-estimate the parameters using the current responsibilities:

$$\mu_q^{new} = \frac{1}{N_q} \sum_{n=1}^N \gamma_n x_n \quad (10)$$

$$\Sigma_q^{new} = \frac{1}{N_q} \sum_{n=1}^N \gamma_n (x_n - \mu_q^{new})(x_n - \mu_q^{new})^T \quad (11)$$

$$\omega_q^{new} = \frac{N_q}{N} \quad (12)$$

with:

$$N_q = \sum_{n=1}^N \gamma_n \quad (13)$$

**Step 4:** Compute the log-likelihood:

$$\ln p(X; \theta) = \sum_{n=1}^N \ln \left\{ \sum_{q=1}^M \omega_q N_q(x_n, \theta) \right\} \quad (14)$$

**Step 5:** Check for the convergence:

If  $|\theta^{new} - \theta| \leq \varepsilon$  or  $|\ln p(X; \theta^{new}) - \ln p(X; \theta)| \leq \delta$  then stop. Otherwise go to **Step 2**.

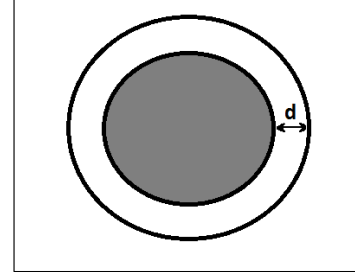


Fig. 2. Cross sectional diagram of a peg-in-hole assembly process showing the peg (the gray), the inlay of the hole (the outer circle), and the clearance  $d$ .

### 3.2. The Spiral Search Path

When the peg misses the hole, then a search path is followed in order to find its accurate position. Before explaining the search path, we need to mention that inspired from a blindfolded human action, one can look for a certain position with closing the eyes if the search is limited to a certain area of a prescribed radius, otherwise the searching objective would be infeasible. Likewise to the force-guided robotic assembly task, the search of the accurate position will be restricted within a certain search area. Suppose that the clearance of the peg-in-hole assembly task, the distance between the peg and the inlay of the hole when centering the peg, is  $d$  (Fig. 2 shows the clearance of a peg-in-hole assembly task). In case the peg misses the hole, then the robot moves the peg in a spiral path on the surface of the environment. Archimedean spiral is used as a search path in order to facilitate the computations of the spiral parameter since the spanning distance between the consecutive turns is constant. Fig. 3 shows a spiral of starting radius  $a$  and spanning distance  $b$ . The  $x, y$  coordinates of the Archimedean spiral shown in Fig. 3 can be described as:

$$x(t) = r(t) \cos(\Psi(t)) \quad (15)$$

$$y(t) = r(t) \sin(\Psi(t)) \quad (16)$$

$r(t)$  is the radius of the spiral turns,  $\Psi(t)$  is the polar angle swept by the path curve,  $a$  is a parameter specifying the outer radius of the spiral path,  $b$  is a parameter specifying the spanning distance between two consecutive turns. It is worth noting that  $\Psi(0)=0$  and it increases linearly with time. The equation of  $r(t)$  is:

$$r(t) = a - b\Psi(t) \quad (17)$$

provided that:

$$r(t) \geq 0 \quad (18)$$

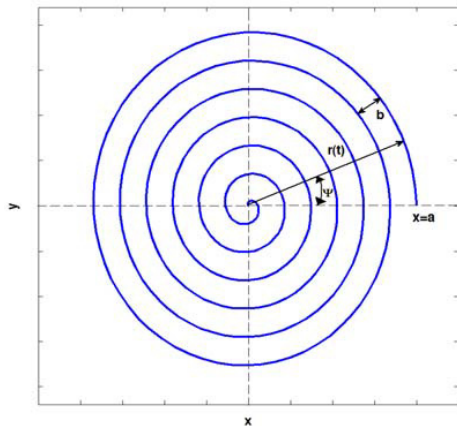


Fig. 3. Archimedean spiral path with spanning distance  $b$  and starting radius of  $a$ .

Hence, the search path will follow concentric circular shapes with linearly decaying radii spanned by a distance of  $b$  and included in circular search zone of radius  $a$ . Thus both  $b$  and  $a$  will determine the shape of the spiral path to be followed. It is worth noting that the value of  $b$  should be chosen such that:

$$b \leq 2d \quad (19)$$

The constraint of (19) will ensure that the hole is swept properly wherever it is located inside the outer circle of Fig. 3.

### 3.3. The Proposed Position Identification Algorithm

As soon as the CS models of the three phases are developed, then one can use them in finding the accurate hole position along with the spiral search path explained above. More specifically, if we start from free space (CS1) then the robot is moved towards the hole. In case of touching the environment with missing the hole, the robot is entered into the searching mode (CS2) until it finds the hole. As soon as CS3 is detected, then the accurate hole position is determined. The proposed search strategy can be summarized by the following algorithm:

- Step 1:** Enter the assembly clearance  $d$  and search radius  $a$ ;  
Enter the value of  $b$  according to (19);
- Step 2:** Enter the CS models of the assembly phases;
- Step 3:** Capture the wrench signals (3);
- Step 4:** If CS1 is detected:  
Approach the uncertain hole position;  
Go to **Step3**;
- Step 5:** If CS2 is detected:  
Implement the spiral search path using (15)-(17);  
Go to **Step3**;
- Step 6:** If CS3 is detected:  
Hole is reached;  
Stop;  
Otherwise go to **Step3**;

Fig. 4 shows the flow chart of the proposed hole position identification strategy. One can see that the positioning of the hole relies only on the captured wrench signals of the manipulated As soon as the models of the three CSs are developed, then one can use them in finding the accurate hole position along with the use of the spiral search path explained above. More specifically, if we start from free space (CS1) then the robot is moved towards the hole. In case of touching the environment with missing the hole, the robot is entered into the searching mode (CS2) until it finds the hole. As soon as CS3 is detected, then the accurate hole position is determined.

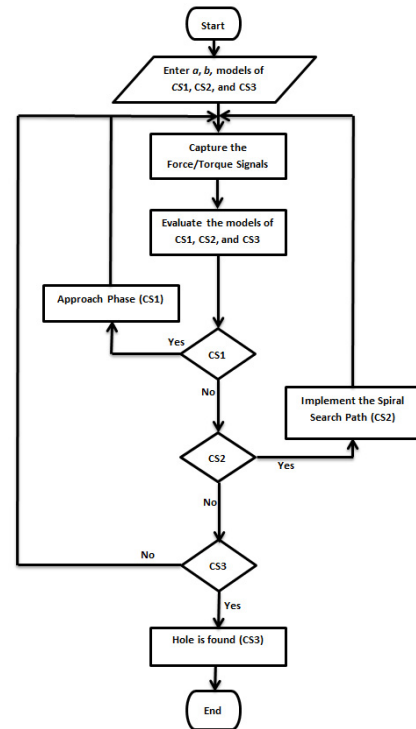


Fig. 4. The flow chart of the proposed hole position identification algorithm.

## 4. Experimental Validation

In order to evaluate the performance of the proposed position identification strategy, a test stand is built that is composed of a KUKA Lightweight Robot (LWR) doing force-guided peg-in-hole assembly task. The clearance of the considered peg-in-hole assembly is  $6.25 \text{ mm}$ . Fig. 1 shows the test stand built for this experiment. More description on the KUKA LWR can be found in [8]. The robot is equipped with a Fast Research Interface (FRI) port that allows researchers of capturing the wrench and pose readings of the manipulated object measured by sensors installed within the robot. The FRI port is connected to a remote PC that performs the computational aspects of the modeling process. The feature of the PC that was used in this test stand is of Intel (R) Core (TM) i5-2540 CPU with 2.6 GHz speed and 4 GB RAM running under a Linux environment. The rate of the communication between the remote PC and the robot, through

the FRI, is 100 Hz. The programming is done through a C++ platform.

From Fig. 1, one can see that the considered peg-in-hole assembly process is composed of three phases; phase 1 in which the robot is in free space, phase 2 that is resulted when the robot misses the hole and implementing the spiral search path, and phase 3 in which the robot places the peg precisely on the hole (peg-on-hole). At the beginning, the robot is programmed to move along those three phases while capturing the wrench signals of the manipulated object. Fig. 5 shows the signals that was obtained when programming the robot to move from free space, to the spiral search path, and finally to the hole. It is worth noting that in capturing the signals of Fig. 5, the spiral path was programmed to last significantly enough to have good and accurate models of the considered phases. The models of those three phases were developed using the EM-GMM CS modeling scheme and then two experiments were conducted as detailed below:

#### 4.1. Experiment 1

In this experiment, the hole is moved in the  $x$ - $y$  plane to an arbitrary unknown position (all Cartesian values are with respect to the robot base). Since the clearance of the assembly is  $6.25\text{ mm}$ , then one can take  $b$  to be any value satisfying (19). In this experiment,  $b$  was taken to be  $5\text{ mm}$ . The outer radius  $a$  was taken to be  $20\text{ mm}$  and the hole is assumed to be within the circle formed by such a radius. Implementing the position identification strategy described in section 3, the values of  $x$  and  $y$  were found to be  $490.665\text{ mm}$  and  $-337.926\text{ mm}$  respectively. The scenario of finding the hole position started in moving the robot from free space and as soon as CS2 is detected then the spiral search path is followed until CS3 is recognized and then the robot stops and the  $x$ - $y$  values are stored/reported for further possible actions. Fig. 6 shows the signals during this experiment and the instant at which CS3 is detected. One can see the excellent CS detection performance resulted in excellent hole position identification. It is worth noting that the choice of  $a$  has a direct effect on the speed of finding out the hole position since larger radius of the search results in more time to survey the whole area. The time measured for finding the hole was found to be  $11.96\text{ sec}$ .

#### 4.2. Experiment 2

The hole is placed arbitrarily in a larger circle of uncertainty and the outer radius  $a$  is chosen to be  $40\text{ mm}$ . The value of  $b$  is kept at  $5\text{ mm}$ . Using the proposed position identification strategy the values of  $x$  and  $y$  were found to be  $502.276\text{ mm}$  and  $-380.943\text{ mm}$  respectively. The captured signals of this experiment along with the model output of phase 3 are shown in Fig. 7. One can notice that as soon as the model of phase 3 is triggered with 1 at the output, the robot is stopped and the values of the  $x$  and  $y$  coordinates are stored. The time required to find the hole in this experiment was measured to be  $37.81\text{ sec}$ . and comparing the time of this experiment with that of experiment 1, one can notice that the searching time was significantly increased when increasing the outer radius of the search circle. Therefore and for the sake of reducing the time required for such position search objective, it is recommended to reduce the radius of the search circle as much as possible so that the searching time is reduced accordingly.

### 5. Conclusion

The problem of the hole position identification in force-guided robotic assembly tasks was addressed. A position identification strategy was proposed for such robotic tasks employing the captured wrench (the Cartesian force and torque) signals of the manipulated object. The proposed identification strategy is composed of two main aspects; detecting the Contact-State (CS) of the robot using the Expectation Maximization-based Gaussian Mixtures Modeling (EM-GMM CS) modeling scheme and a spiral search path. The EM-GMM CS modeling scheme adds the required abstract knowledge of the environment and the spiral search path helps in finding the hole position if the peg misses the hole during the mating process by sliding on the surface of the environment until the peg-on-hole phase is detected. Experiments are carried out on a KUKA Lightweight Robot (LWR) doing a typical peg-in-hole assembly process. Two distinct positions are studied and the excellent performance of the hole position identification is shown.

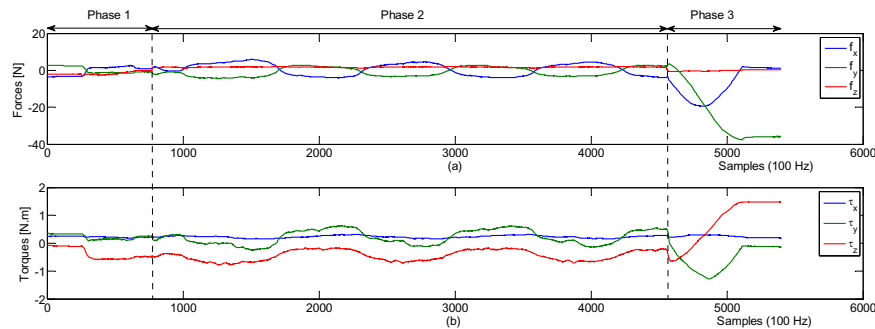


Fig. 5. The models training signals: (a) Cartesian forces; (b) Torques around the Cartesian axes.

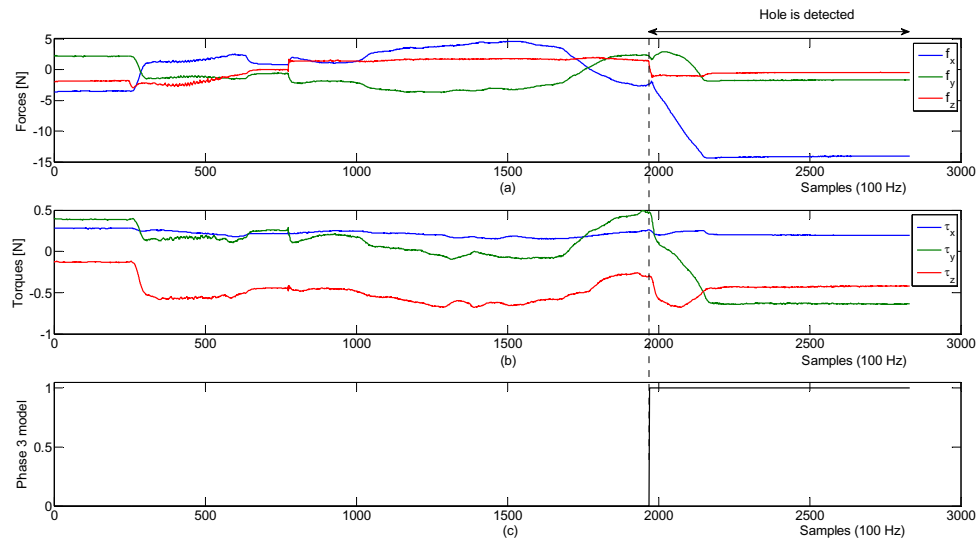


Fig. 6. Experiment 1 signals: (a) Cartesian forces; (b) Torques around the Cartesian axes; (c) Phase 3 model output.

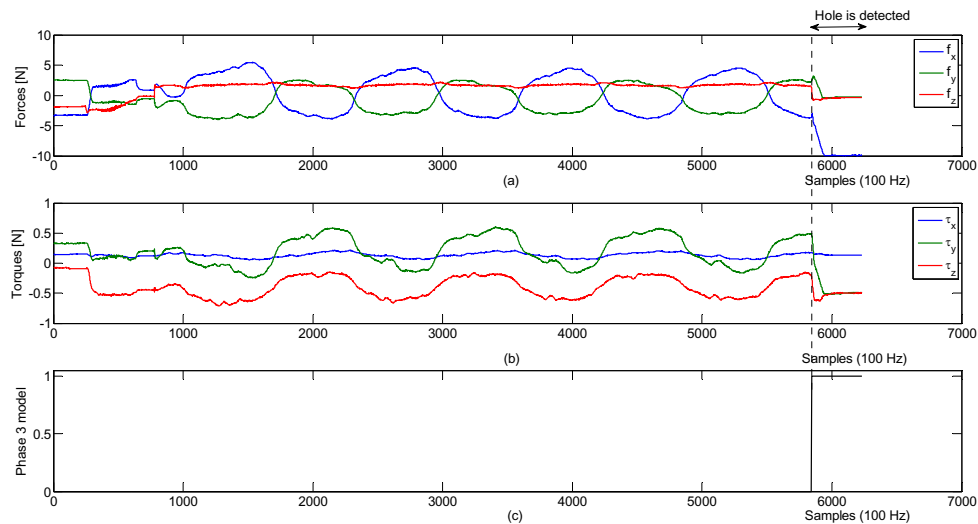


Fig. 7. Experiment 2 signals: (a) Cartesian forces; (b) Torques around the Cartesian axes; (c) Phase 3 model output.

## Acknowledgements

This work is supported by the Fonds National de la Recherche (FNR) in Luxembourg under grant no. AFR-2955286.

## References

- [1] Chhatpar S.R., Branicky M.S., 2001. Search strategies for peg-in-hole assemblies with position uncertainty. Proc. 2001 IEEE/RSJ Int. Conf. Intell. Robot. Syst., Hawaii-USA, 29 Oct.-3 Nov., p.1465-1470.
- [2] Chhatpar S.R., Branicky M.S., 2003. Localization for robotic assemblies with position uncertainty. Proc. 2003 IEEE/RSJ Int. Conf. Intell. Robot. Syst., Las Vegas-USA, 27-31 Oct., p. 2534-2540.
- [3] Chhatpar S.R., Branicky M.S., 2005. Particle filtering for localization in robotic assemblies with position uncertainty. Proc. 2005 IEEE/RSJ Int. Conf. Intell. Robot. Syst., Alberta-Canada, 2-6 Aug., p. 3610-3617.
- [4] Kim Y.-L., Kim B.-S., Song J.-B., 2012. Hole detection algorithm for square peg-in-hole using force-based shape recognition. Proc. 8<sup>th</sup> IEEE Int. Conf. Autom. Sci. Eng., Seoul-Korea, 20-24 August, p. 1074-1079.
- [5] Kim Y.-L., Song H.-C., Song J.-B., 2014. Hole detection algorithm for chamferless square peg-in-hole based on shape recognition using F/T sensor. Int. J. Prec. Eng. Manuf., vol. 15, no. 3, p. 425-432.
- [6] Jasim I.F., Plapper P.W., 2014. Contact-state recognition of compliant motion robots using expectation maximization-based Gaussian mixtures. Proc. Joint 45<sup>th</sup> Int. Symp. Robot. and 8<sup>th</sup> German Conf. Robot., Munich-Germany, 2-3 June, p. 56-63.
- [7] Bishop C.M., 2006. Pattern Recognition and Machine Intelligence. Springer.
- [8] Lightweight Robot 4+ Specification, Version: Spez LBR 4+ V5 en, KUKA Roboter GmbH, 22 Dec., 2011.